Stability and Bifurcations of the Wake Behind a Ring: A Computational and Experimental Comparison

G. J. Sheard [1] , M. C. Thompson[1], T. Leweke [2] , K. Hourigan[1]

Summary

The wakes behind open rings of two different aspect ratios are computed using a spectral-element method, and the stability of the solutions are analysed by the application of a linear stability analysis. The predicted instabilities are compared with the computed three-dimensional flows and with experimentally obtained dye visualisations. The flows computed at the chosen aspect ratios show that the bifurcations from steady axisymmetric flow produce remarkably different wakes. This phenomenon is related to the existence of a transition aspect ratio that delineates annular and cylinder-like wakes at small and large aspect ratios, respectively.

Background: The Stability of Bluff-Body Flows

The subject of instability and the bifurcation of fluid flows is as rich as it is diverse. The motion of a fluid around even the simplest of geometries is governed by the mathematically formidable Navier–Stokes equations; a set of non-linear partial differential equations for which analytical solutions to practical flows are rare.

It has been understood for more than a century that the non-linearity of the Navier–Stokes equations is governed by the dimensionless Reynolds number parameter $Re = VL/\nu$ [1], where V and L are velocity and length scales, respectively, and ν is the kinematic viscosity. Thus, even for a fluid constrained by constant boundary-conditions, a wide range of flows are described through alteration in the Reynolds number. Typically, with an increase in Reynolds number, a fluid experiences several transitions from steady laminar flow. These include transitions which mark the development of unsteady flow, three-dimensional flow, and turbulent flow. These transitions have been well-documented for some classical flows, which include the transition from laminar to turbulent flow in tubes [1], and the development of turbulent flow in the boundary-layer above a flat plate [2].

During the last century, development in fields such as automotive and aeronautical engineering drove the need for an improved understanding of the flow around bluff and streamlined bodies. This paper is concerned with the canonical geometries for bluff-body research, a sphere and a straight circular cylinder. A sphere and a circular cylinder are natural choices as reference geometries for the study of bluff-body flows, as they are simply a circular body of revolution, and a circular body of translation, respectively.

[1]Fluids Laboratory for Aeronautical and Industrial Research (FLAIR), Department of Mechanical Engineering, Monash University, Melbourne, Victoria 3800, AUSTRALIA

[2]Institut de Recherche sur les Phénomènes Hors Équilibre (IRPHÉ), UMR 6594 CNRS / Universités Aix-Marseille I & II, 12 avenue Général Leclerc, F-13003 Marseille, FRANCE

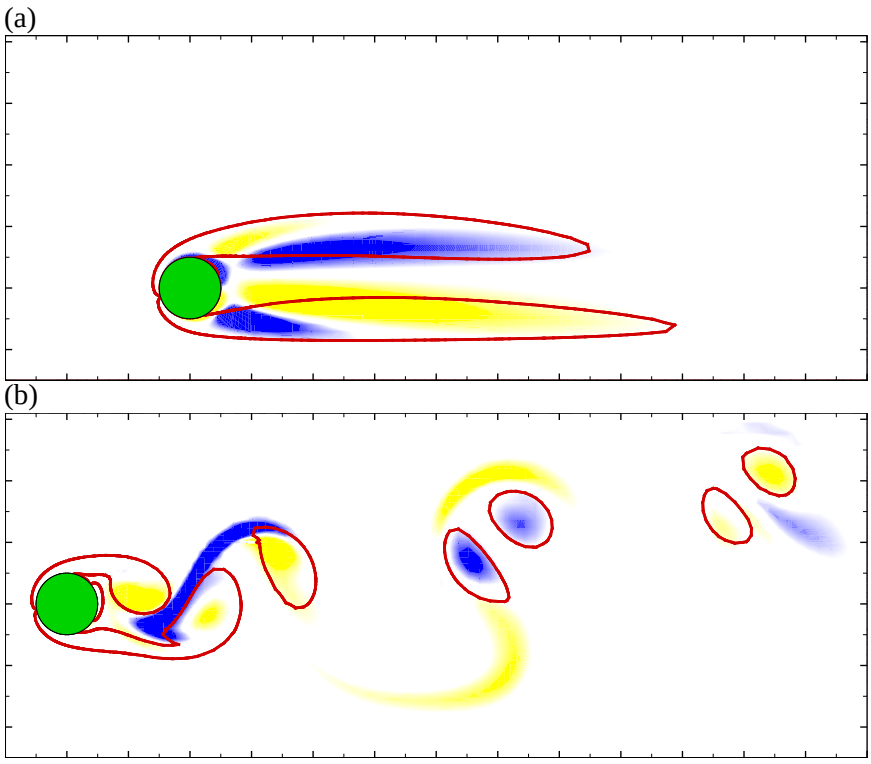

Figure 1: Comparison between the perturbation fields of the first-occurring non-axisymmetric instability in the wakes behind rings with $A_R = 3$ (a) and $A_R = 5$ (b). Red contour lines indicate the location of annular vortices in the wake, and flooded yellow and blue contours highlight regions of negative and positive streamwise perturbation field vorticity. The ring, coloured green, is located at the left of each frame, and flow is from left to right.

Transitions in the Wake of Spheres and Circular Cylinders

The transitions in the flows past a sphere and a circular cylinder with an increase in Reynolds number is initiated by separation of the boundary-layer around the body [3][4], which causes a region of recirculating fluid to form in the wake. Computational stability analyses have shown that these steady symmetrical recirculation bubbles become unstable through a regular non-axisymmetric bifurcation at $Re \approx 210$ for the flow past a sphere [5], and an unsteady two-dimensional bifurcation at $Re \approx 46$ for the flow past a circular cylinder [6][7]. Subsequent bifurcations occur in the wakes at higher Reynolds numbers. Most notably, for the flow past a sphere beyond $Re \approx 272$, the steady non-axisymmetric wake bifurcates to an unsteady flow [8][9] which produces the vortex-loop wake observed years earlier [10][11][12]. In addition, the classic two-dimensional Kármán vortex street

(a)

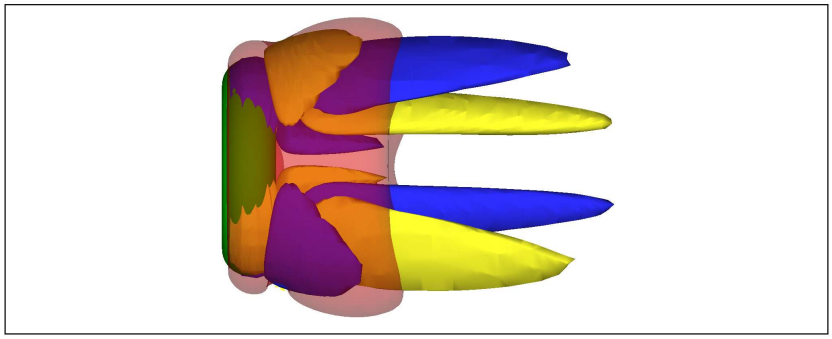

(b)

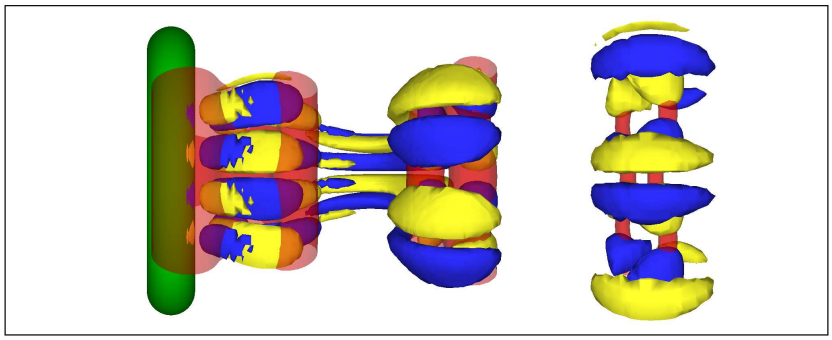

Figure 2: Comparison between the non-axisymmetric wakes computed for the flow past rings with $A_R = 3$ (a) and $A_R = 5$ (b) at $Re = 115$ and $Re = 170$, respectively. Wakes are visualised with streamwise vorticity isosurfaces (yellow and blue isosurfaces show negative and positive vorticity, respectively), and a red isosurface of pressure approximates the location of the recirculation zone in the wake. The ring, coloured green, is located at the left of each frame, and flow is from left to right.

(visualisations may be found in [13][14]) becomes unstable to a spanwise-periodic three-dimensional instability with a wavelength of approximately $3.9d$ (where d is the cylinder diameter) [15] known as Mode A. A set of complex non-linear interactions follow, including the evolution of a secondary instability with a wavelength of approximately $0.8d$ [16] known as Mode B, before the wake becomes turbulent through the evolution of fine-scale vortices beyond $Re \approx 300$ [17][18].

The Ring: A Continuous Link Between Spheres and Circular Cylinders

The differences between the bifurcation scenarios for the flows past a sphere and a circular cylinder are stark. In order to answer the question as to how the geometry played a role in the bifurcation process for bluff-body flow, a computational stability analysis [19]

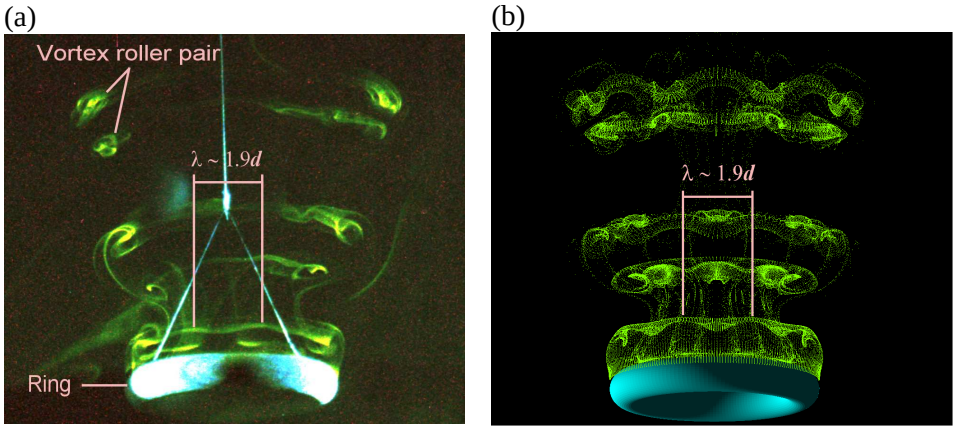

Figure 3: Comparison between an experimental dye-visualisation (a) and a numerical simulated-particle computation (b) which shows evidence of the subharmonic Mode C instability in the wake. Note the azimuthal wavelength of the non-axisymmetric wake structures of approximately $\lambda_d \approx 1.7d$. The ring is located at the bottom of each frame, and flow is upwards.

and a complementary study of the computed non-axisymmetric flow [20] past rings were performed. The ring is ideal for such a study as it alters continuously with an increase in an aspect ratio parameter (A_R) from a solid body of revolution ($0 \leq A_R \leq 1$), to an open ring ($A_R > 1$), before finally approaching a circular cylinder local to the ring cross-section as $A_R \to \infty$.

One interesting aspect of the results of the previously mentioned studies was the prediction of a critical aspect ratio which marked an abrupt transition in flow regimes, from axisymmetric sphere-like transition modes for $0 \leq A_R \lesssim 4$, and cylinder-like transition modes for $4 \lesssim A_R < \infty$. The computations reported in this paper highlight the large variation in flow regimes between aspect ratios $A_R = 3$ and $A_R = 5$, which straddle the critical aspect ratio.

In the present study, a spectral-element method was employed to compute the unsteady incompressible Navier–Stokes equations in cylindrical-polar coordinates. This choice of coordinate system facilitated simple modelling of the ring, which is simply a circle in the z–r plane, rotated in the θ-direction around the symmetry axis. To discretise the flow, a mesh was constructed over the z-r plane, and appropriate boundary conditions were selected, as described in [19] and [20]. A linear stability analysis was performed, which used numerical formulation successfully applied in [19]. Non-axisymmetric flow was modelled by incorporating an azimuthal Fourier expansion of the velocity and pressure fields, which enforced periodic boundary conditions at the azimuthal boundaries.

The First-Occurring Non-Axisymmetric Transition in the Flow past Rings

Results are now presented for computations of the flow past rings with $A_R = 3$ and $A_R = 5$. Compare, for example, the perturbation fields presented in figure 1(a) and 1(b), which were obtained from a linear stability analysis of the dominant non-axisymmetric mode of the axisymmetric wakes. In figure 1(a), the first-occurring non-axisymmetric instability is shown, which was predicted to occur through a regular bifurcation with azimuthal mode number $m = 2$ ($\lambda_d \approx 3.1d$). In figure 1(b), the first-occurring non-axisymmetric instability is shown, which was predicted to occur through a subharmonic bifurcation of the axisymmetric periodic vortex street, with an azimuthal mode number $m = 10$ ($\lambda_d \approx 1.6d$).

In order to verify that the predicted linear instability modes match the computed saturated non-axisymmetric wakes, non-axisymmetric computations were performed. Isosurface plots of the resulting wakes are reproduced here in figure 2. Figure 2(a) shows the steady non-axisymmetric wake which evolved from the Mode III instability, and figure 2(b) shows the $2T$-periodic wake which evolved from the Mode C instability [20]. Observe the contrast in the topology of the streamwise vorticity isosurfaces between the two rings, despite the geometric similarity between the rings.

To verify the physical relevance of the computed non-axisymmetric instabilities reported in this study, experimental dye-visualisation was performed on a buoyant ring with an aspect ratio $A_R \approx 4.9$. The ring was towed vertically downward in a water tank, and the dye was illuminated with a laser light source. The experiments highlighted the robustness of the non-axisymmetric Mode C instability to the non-linear longer-wavelength disturbances associated with physical flows.

The experimental dye-visualisation is compared to non-axisymmetric computations of the saturated Mode C instability in the wake of a ring with $A_R = 4.9$ in figure 3. For visualisation in the numerical computations, simulated particles were injected into the flow field close to the separation points on the downstream surface of the ring. This provided a close approximation of the convection of dye into the wake in experiment. A non-axisymmetric waviness of the annular vortex rollers can clearly be observed with a wavelength of approximately $1.9d$. This suggests that the observed mode evolved from the Mode C instability.

Conclusion

In conclusion, the stability and bifurcations of bluff-body flows provide a complex and often surprising diversity at low Reynolds numbers for different geometries. This study has shown that for rings which differ in slenderness by just 30%, the route to unsteady non-axisymmetric flow occurs through a completely different set of bifurcations.

Reference

1. Reynolds, O. (1883): "An Experimental Investigation of the Circumstances Which Determine Whether the Motion of Water Shall be Direct of Sinuous, and of the Law of Resistance in Parallel Channels", *Phil. Trans. R. Soc.*, Vol. 174, pp. 935–982.
2. Dryden, H.L. (1937): "Airflow in the Boundary Layer near a Plate", *NACA Tech.*

Report 562, pp. 339–364.

3. Taneda, S. (1956): "Experimental Investigation of the Wake Behind a Sphere at Low Reynolds Numbers", *J. Phys. Soc. Japan*, Vol. 11(10), pp. 1104–1108.
4. Taneda, S. (1956): "Experimental Investigation of the Wakes Behind Cylinders and Plates at Low Reynolds Numbers", *J. Phys. Soc. Japan*, Vol. 11(3), pp. 302–307.
5. Natarajan, R. and Acrivos, A. (1993): "The Instability of the Steady Flow Past Spheres and Disks", *J. Fluid Mech.*, Vol. 254, pp. 323–344.
6. Provansal, M., Mathis, C. and Boyer, L. (1987): "Bénard-von Kármán Instability: Transient and Forced Regimes", *J. Fluid Mech.*, Vol. 182, pp. 1–22.
7. Dušek, J., Le Gal, P. and Fraunié, P. (1994): "A Numerical and Theoretical study of the First Hopf Bifurcation in a Cylinder Wake", *J. Fluid Mech.*, Vol. 264, pp. 59–80.
8. Ghidersa, B. and Dušek, J. (2000): "Breaking of Axisymmetry and Onset of Unsteadiness in the Wake of a Sphere", *J. Fluid Mech.*, Vol. 423, pp. 33–69.
9. Thompson, M. C., Leweke, T. and Provansal, M. (2001): "Kinematics and Dynamics of Sphere Wake Transition", *J. Fluids Struct.*, Vol. 15, pp. 575–585.
10. Magarvey, R. H. and Bishop, R. L. (1961): "Wakes in Liquid-Liquid Systems", *Phys. Fluids*, Vol. 4(7), pp. 800–805.
11. Magarvey, R. H. and Bishop, R. L. (1961): "Transition Ranges For Three-Dimensional Wakes", *Canadian J. Phys.*, Vol. 39, pp. 1418–1422.
12. Magarvey, R. H. and MacLatchy, C. S. (1965): "Vortices in Sphere Wakes", *Canadian J. Phys.*, Vol. 43, pp. 1649–1656.
13. Zdravkovich, M. M. (1969): "Smoke Observations of the Formation of a Kármán Vortex Street", *J. Fluid Mech.*, Vol. 37, pp. 491–496.
14. Van Dyke, M. (1982): *An Album of Fluid Motion*, The Parabolic Press.
15. Barkley, D. and Henderson, R. D. (1996): "Three-Dimensional Floquet Stability Analysis of the Wake of a Circular Cylinder", *J. Fluid Mech.*, Vol. 322, pp. 215–241.
16. Henderson, R. D. (1997): "Non-Linear Dynamics and Pattern Formation in Turbulent Wake Transition", *J. Fluid Mech.*, Vol. 352, pp. 65–112.
17. Bloor, M. S. (1964): "The Transition to Turbulence in the Wake of a Circular Cylinder", *J. Fluid Mech.*, Vol. 19, pp. 290–304.
18. Williamson, C. H. K. (1996): "Three-Dimensional Wake Transition",*J. Fluid Mech.*, Vol. 328, pp. 345–407.
19. Sheard, G. J., Thompson, M. C. and Hourigan, K. (2003): "From Spheres to Circular Cylinders: The Stability and Flow Structures of Bluff Ring Wakes", *J. Fluid Mech.*, Vol. 492, pp. 147–180.
20. Sheard, G. J., Thompson, M. C. and Hourigan, K. (2004): "From Spheres to Circular Cylinders: Non-Axisymmetric Transition in the Flow past Rings", *J. Fluid Mech. (In press)*.